A CONCEPT FOR A NOVEL POLYMER EXTRUDER PART I: ACTIVE GROOVED FEED SECTION

Mirosław Ferdynus[1*], Peter Chorovsky[2], Hubert Dębski[3], António Gaspar-Cunha[4]

[1,3] Lublin University of Technology, Faculty of Mechanical Engineering, Lublin, Poland; m.ferdynus@pollub.pl, h.debski@pollub.pl
[2] SEZ Krompachy a.s., Krompachy, Slovakia; peter.chorovsky@sez-krompachy.sk
[4] Institute for Polymer and Composites, University of Minho; agc@dep.uminho.pt
[*] Correspondence: e-mail: m.ferdynus@pollub.pl, 20-618 Lublin, 38 D Nadbystrzycka Str, Poland

Key Words: *Polymer extruder, Grooved feed section, Polymers, Granulates, Finite element method.*

Abstract

This paper presents a novel concept for an extruder to be used with plastics and polymer composites, especially in the food industry. The design solutions include a grooved feed section with adjustable geometric parameters, which makes it possible for dynamic adjustment of the depth, inclination angle and number of grooves used for granulate transport during continuous operation of the machine. The proposed grooved feed section concept facilitates optimum performance, and is adjustable to suit the general parameters of production. The scope of our study also included the numerical strength and thermal analysis of the designed grooved feed section, conducted using the finite element method. Numerical calculation involved a coupled temperature-displacement analysis which constituted a geometrically and physically non-linear problem. The results corroborated the achievement of satisfactory strength for the structural elements of the grooved feed section in the extruder and demonstrated the suitability of the adopted solution in terms of temperature distribution in the parts of the machine, as well as the correct concept of the designed cooling system. The numerical tool used was the ABAQUS® commercial program.

1. INTRODUCTION

The growing requirements concerning polymer materials, legal regulations, and market competition result in the emergence of new materials and composites with various fillers, e.g. organic fillers from renewable sources or nanofillers, which in many cases become hard-to-process mixtures with specific processing properties, such as high molecular weight, high viscosity and low coefficients of friction, e.g. UHMWPE, or classic polymers (PE, PP) filled with short fibre or powder. Their processing using standard plasticising systems in processing machines, mainly extruders, is tending to become ineffective, unstable, and uncompetitive. In the literature, there are several publications which demonstrate the impact of the size and shape of granulate on the effectiveness of the extrusion process. Sikora JW. and Samujło B. [1] demonstrated that it is best to feed the plasticising system in a W-25 extruder with a plasticised poly(vinyl chloride) granulate characterised by similar values of granule length and diameter, and the process being carried out with the highest-possible rotational speed of the screw. Other granule dimensions did not facilitate such good performance. On the other hand, Jia M.-Y and Pa L. et al. developed a novel pellet-size physical model to guide the available design of the barrel channel geometry for positive conveying [2]. The possibility of selecting the geometric properties of the granulate to achieve the most optimal effectiveness of extrusion was demonstrated. However, it is also possible to take the opposite approach, by adapting the design of the plasticising system to the size of the granulate fed into the extruder.

The impact of the geometric properties of the feed section on the output and pressure of the material in the extruder's plasticising system was also described and referred to in the literature.

In this regard, extruders with a grooved feed section perform the best, and facilitate a several-dozen-percent increase in performance and pressure. All extruders of this kind have grooved feed sections with unchanged designs. Wortberg [3] determined that the experimental data presented in his paper show that grooved barrel conveying can substantially enhance the performance of screws in single screw extruders. Furthermore, the improvements in through rate and melt temperature control are evident for a broad range of resins, such as PA, LDPE, and PVDF. Further developments, like gearless extruders with high screw speeds or melt separation techniques, may be based on an optimized grooved feed section design. Sasimowski et al. demonstrated that the application of a grooved feed section could significantly increase the performance of low-density polyethylene processing [4], while Bruce A. Davis et al. noted that the performance of an extruder with a 45 mm screw and a grooved feed section was comparable to that of extruders with a screw diameter of 90 mm and smooth barrels [5].

The quality of the extrudate is confirmed by the degree of mechanical and thermal homogenisation of the material, which in many cases requires the application of additional devices, which take the form of static mixers installed in the process line. This is of particular importance in the case of filled plastics, including those filled with nanofillers, which can in many cases be subject to agglomeration, thus decreasing the quality of the obtained products. Głogowska and Sikora [6] stated that the modification of polymers by a wide variety of fillers causes numerous changes in the processing, mechanical properties, and morphology of product structure, while admitting, as have other researchers [7, 8] that the properties depend, first and foremost, on good mixing.

Thus, innovative plasticising systems were designed for a single-screw extruder with an adjustable grooved feed section. They facilitate the introduction of changes to the design features, such as the number of grooves and groove depth during extrusion, and adjusting these parameters to the variable granulate size. The main benefits of using an active grooved feed section during extrusion is that without the need to stop the operation of the extruder or change the operating parameters, you can affect the extrusion process by adapting it to the variable dimensions of the granulate and maintain a constant performance regardless of the properties of the extruder feeding material.

Before commercialising the developed solutions, it is recommended to carry out design and optimisation processes, which should include virtual modelling with an analysis of the kinematic parameters in order to eliminate any possible conflicts between the moving parts of the machine. An FEM numerical simulation follows the optimisation of the design features, which makes it possible to evaluate the proposed design in terms of its strength thermal properties, thus allowing the selection of an optimal solution without costly and extended testing.

The objective of this paper is to present a novel concept for an extruder plasticising system featuring an innovative adjustable grooved feed section, facilitating the adjustment of groove depth, inclination angle and number of grooves during the extrusion process. This concept is fully functional and tested in terms of strength and thermal properties, i.e. ready for further stages of commercialisation.

2. CONCEPT FOR THE EXTRUDER'S FEED SECTION

The feed section is a "cold" part of the extruder, intended for the supply and transport of a plastic granulate, which is then plasticised in the "hot" section of the extruder. In order to ensure optimal granulate transportation conditions, in terms of achieving the desired performance of the machine, the feed section was designed as a grooved type. This concept entailed making internal grooves in the extruder barrel to facilitate the required compression of the granulate and allow an increase in the volume of the transported material by increasing the internal volume of the machine. The proposed concept facilitates changes in the internal space through the use of variable-depth grooves. These changes can be adjusted on an ongoing basis during the operation of the extruder,

which makes it possible to obtain optimal extrusion parameters. The concept of a feed section with an adjustable grooved section is presented in Figure 1.

The primary and most innovative component of the machine is the main sleeve (1), around which the extruder screw rotates. The main sleeve has closely matching slots with four segments (3) seated therein, which can rotate around the axis of the pivots (7). The inclination angle of the segments, which facilitates the maximum depth of the grooves, is set using the special adjusting screw (8) and nut (9) mounted in the support (4). Figure 2a presents (as a cross-section) the machine without grooves, while Figure 2b presents the machine with grooves.

The main sleeve (1) is encased in the barrel (2) with a specially designed cooling system. Cooling of the feed section is crucial for correct performance of the feeding process. In this section of the extruder, the granulate should be received by the plasticising system, but it should not plasticise. In addition, a cooling disc (5) is installed on the front surface of the sleeve. It serves as a thermal barrier, separating the feed section of the extruder (which should remain cold) from the plasticising section (which is hot). The designed cooling unit is composed of two circuits: the main line cooling the extruder's feed section (dark blue) and the channels cooling the separating disc (blue). The cooling system is presented in Figure 3.

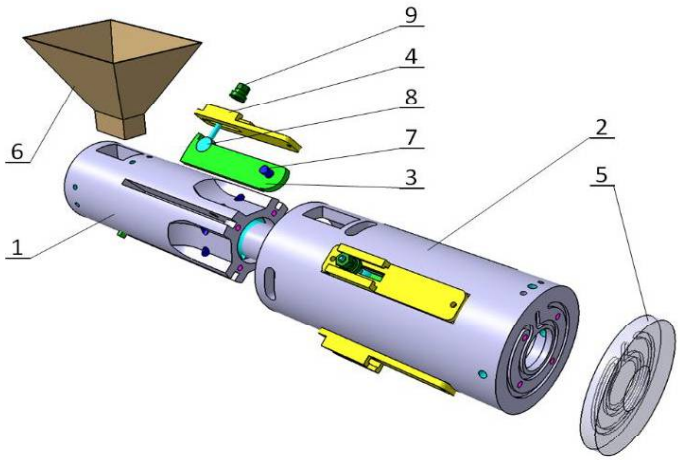

Fig. 1. Conceptual design - exploded view: 1 – main sleeve, 2 – barrel, 3 – moving segment, 4 – support, 5 – separating cooling disc, 6 – hopper, 7 – rotational pivot, 8 – adjusting screw, 9 – special nut

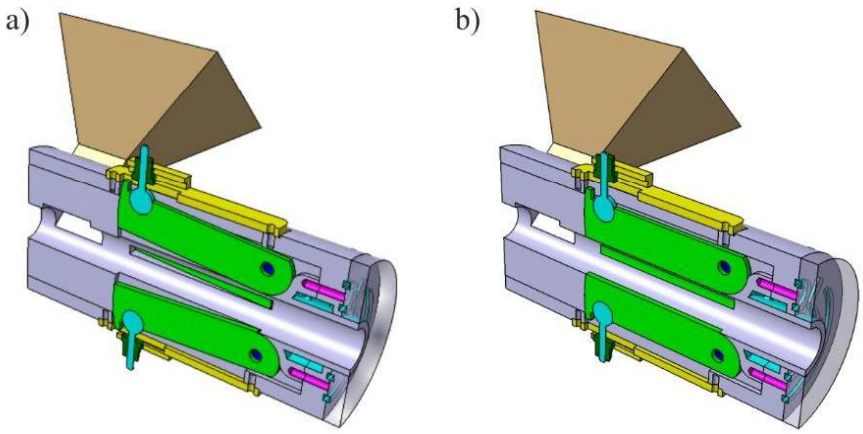

Fig. 2. Conceptual design: a) in the closed position, b) open position

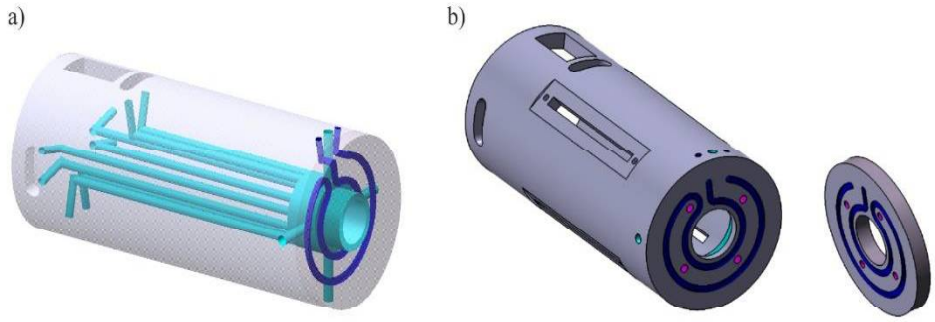

Fig. 3. Cooling ducts in the conceptual design

3. NUMERICAL ANALYSIS OF THE DESIGN

3.1. Methodology of the numerical calculations

Numerical calculations were carried out using the finite element method [9, 10]. The scope of numerical simulations of the structural elements of the extruder's grooved section encompassed a coupled temperature-displacement analysis, which combined the static strength analysis and thermal analysis, facilitating the determination of stress and temperature distribution in the structure in question [11–14]. The basic formula for the fully coupled thermal-stress analysis can be expressed as*:*

$$\begin{bmatrix} K_{uu} & K_{u\theta} \\ K_{\theta u} & K_{\theta\theta} \end{bmatrix} \begin{Bmatrix} \Delta_u \\ \Delta_\theta \end{Bmatrix} = \begin{Bmatrix} R_u \\ R_\theta \end{Bmatrix}, \tag{1}$$

where Δ_u and Δ_θ are the respective corrections to the incremental displacement and temperature, K_{ij} are the submatrices of the fully coupled Jacobian matrix, while R_u and R_θ are the mechanical and thermal residual vectors, respectively. Solving this system of equations requires the use of a non-symmetric matrix storage and solution scheme. Furthermore, the mechanical and thermal equations must be solved simultaneously. The method provides quadratic convergence when the solution estimate is within the radius of convergence of the algorithm.

The numerical calculations constituted a non-linear geometric and physical problem, based on the incremental iterative Newton–Raphson method [15–19]. The numerical tool used was a commercial finite element method package – the ABAQUS® program.

3.2 Discrete model of the extruder's grooved feed section

The discrete model of the extruder's grooved feed section was created based on a geometric model prepared using the Catia V5 software. The discretisation of the geometric model was carried out using C3D10 tetragonal solid elements, which were 10-node elements with a second order shape function and complete integration, and solid C3D8R hexagonal elements, which were 8-node elements with a first order shape function and reduced integration. In addition, C3D10MT tetragonal elements (10-node elements with a second order shape function) and C3D20MT hexagonal elements (20-node elements with a second order shape function) were used, including the thermal analysis, taking the thermal degree of freedom into consideration in the numerical analysis. The applied method of structure discretisation resulted in the creation of a discrete model containing 288058 finite elements and 501818 nodes. This allowed the authors to solve the numerical problem with 2594808 non-linear equations in the coupled analysis

An elastic-plastic model of the material with properties corresponding to those of 40HM steel (assumed for the material properties presented in Table 1) was defined for all structural elements in the devised discrete model.

Tie interactions were defined in the discrete model in order to ensure the required connections between the mating structural elements. These interactions ensured permanent connection of the finite element meshes, by connecting all degrees of freedom on the touching surfaces of these elements. This made it possible to model the capacity for smooth transfer of loads and displacements between the connected structural elements.

In the case of mating structural elements, which took into account mechanical and thermal interactions, contact interactions were applied, facilitating the modelling of the mechanical interactions of the mating elements in the normal and tangential directions, and also allowing the ability to transfer heat on the interaction surfaces between these elements.

Table 1. Mechanical and thermal properties of 40HM steel

Young's modulus E [Pa]	Poisson's ratio [-]	Yield strength R_e [Pa]	Tensile strength R_m [Pa]	Elongation at break [%]	Density ρ [kg/m^3]	Coefficient of linear expansion [-]	Thermal conductivity coefficient λ [W/(m·K)]	Specific heat [J/(kg·K)]
2.1e+11	0.3	8.8e+11	1.03e+12	10	7860	1.2e-5	58	450

The definition of the boundary conditions of the numerical model was met by fixing the nodes located on the specific surfaces of the model, blocking their displacement (translational degrees of freedom of the nodes located on those surfaces) in three directions – X, Y, and Z. The numerical model fixing was carried out by restraining the rear face of the body by blocking all translational degrees of freedom and on the inner edge of the opening of the front face by blocking displacements in the axial direction of the barrel. Figure 4 presents the numerical model of the extruder's grooved section with marked boundary conditions.

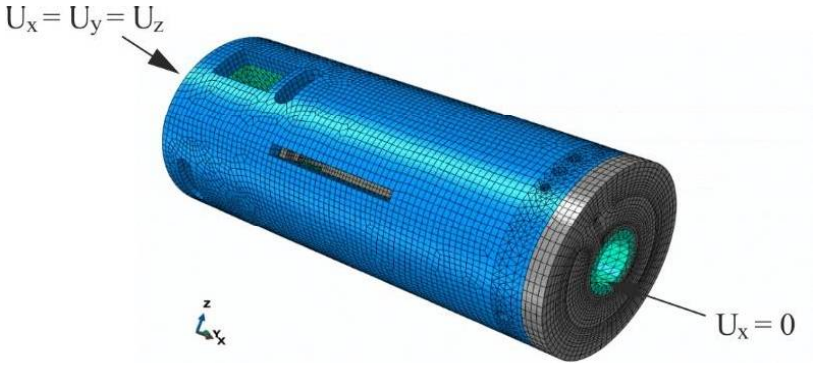

Fig. 4. Discrete model of the extruder's grooved feed section

The load on the numerical model corresponding to continuous operation of the extruder was 18.000s, and included the mechanical and thermal loads. The mechanical load imitated the pressure caused by the extruder's screw transporting the granulate. In this case, the exponential distribution of pressure along the length of the grooved section, LR = 100 mm, was determined with a maximum value (at the end of the section from the filling end) of p = 10 MPa. Figure 5 shows the introduction of pressure into the structure of the grooved section.

The temperature generated through friction between the granulate transported by the screw and the walls of the extruder's grooved feed section formed a thermal load. In the thermal calculation, the exponential distribution of temperature was determined along the length of the grooved section,

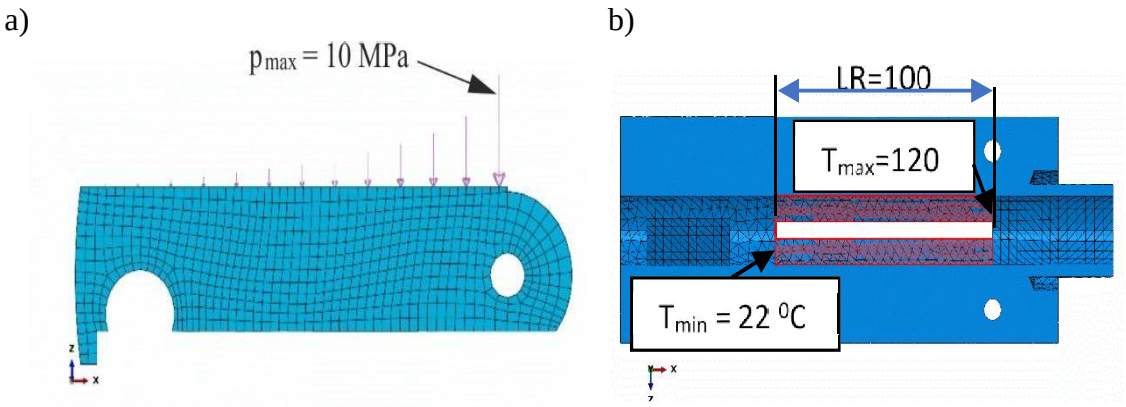

Fig. 5. Loads on the grooved section elements: a) mechanical load, b) thermal load

LR = 100 mm, with a maximum value (at the end of the section from the filling end) of T = 120°C. The initial temperature of the numerical model was assumed at T_0 = 22°C. Figure 5b shows a diagram of the introduction of the temperature load. In addition, thermal analysis involved liquid cooling systems, with the liquid temperature of T_c = 10°C. Figure 6 shows the diagram of loading the discreet model with the cooling liquid temperature.

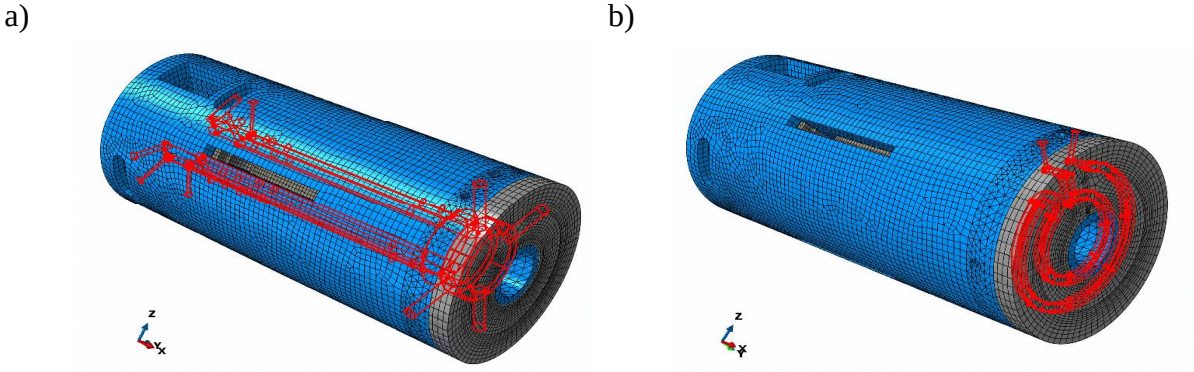

Fig. 6. Diagram of loading with the cooling liquid temperature: a) cooling the grooved section body, b) front cooling disc

4. RESULTS AND DISCUSION

The proposed concept for the extruder's grooved section with variable geometric groove parameters demonstrated an increase in extruder performance as regards the processing of low-density polyethylene, when compared with regular structural solutions for feed systems. This is confirmed by the distributions of material pressure along the length of the plasticising system, calculated for a sample screw speed of 120 rev/min and presented in Figure 7.

The graph was obtained using an author's calculation program. For calculations, it was assumed that the screw has a diameter of 25 mm and the L/D ratio is 25. The lengths of the feed, compression and metering zones are 8D, 8D and 9D, respectively. The active grooved area is 100 mm long. The internal diameter of the screw is 16.6 mm and 22.0 mm, respectively for the feed and metering zones. The properties of low density polyethylene Malen E FGAN 18-D003 from

Basell were used for calculations. The viscosity was obtained experimentally using a capillary rheometer.

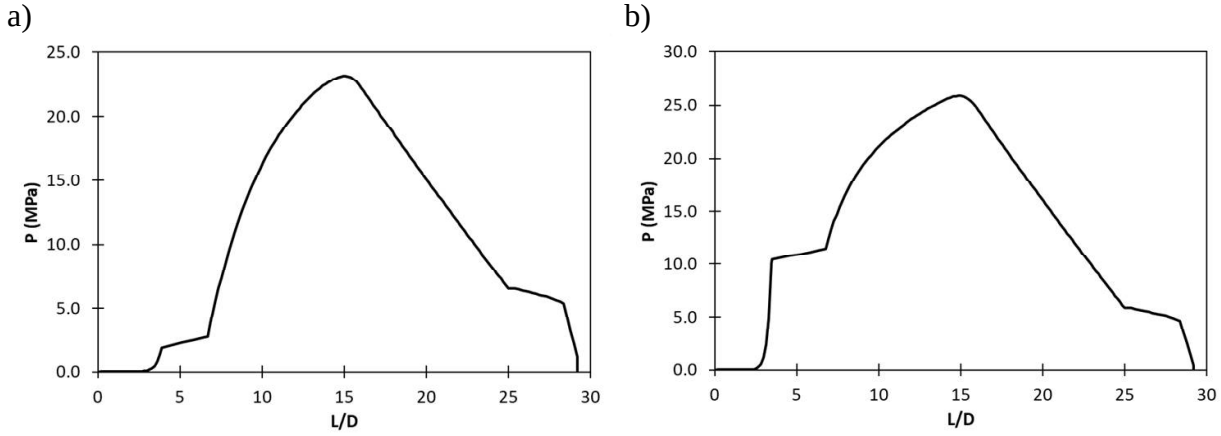

Fig. 7. Distributions of material pressure along the length of the extruder's plasticising system: a) barrel without grooves, b) barrel with grooves

The graph shows the calculated pressure profile along the extruder taking into account the screw geometry, the polymer properties and the operating conditions. The calculations were made considering the complete process, from the hopper until the polymer emerges trough the die. For that purpose all the functional zones of the plasticising process were considered, such as, the solids conveying by gravity in the hopper, the solids conveying in the first turns of the screw due to the friction between the polymer pellets and the screw and barrel walls, the delay zone were a melt film near the barrel wall exists, the melting process taking into account a five zone model and the melt conveying in the screw and in the die. The calculations were made using a numerical method based in finite differences.

Compared to a barrel without grooves, in a barrel with grooves, the pressure increase of the polymer is very intense and it reaches a value several times higher over a short length of the plasticizing system, also the polymer will achieve a higher maximum pressure, which results in stabilization and increase of the polymer flow.

The favourable characteristics of the material pressure distribution along the length of the plasticising system confirm the increase in the processing performance as a result of the application of the grooved section, which proves the innovativeness and favourable properties of the proposed concept of a feeding system for a single-screw extruder, therefore serving as a basis for the commercialisation of this new structural solution. In order to verify the correctness of the designed grooved section, the strength and rigidity of the structural elements were analysed based on reduced stress distributions, determined in accordance with the Huber-Mises-Hencky (HMH) strength hypothesis. A general view of the distribution of reduced stress for mechanical load (with pressure) against a deformation model is presented in Figure 8. The values of pressure are expressed in Pa.

a)

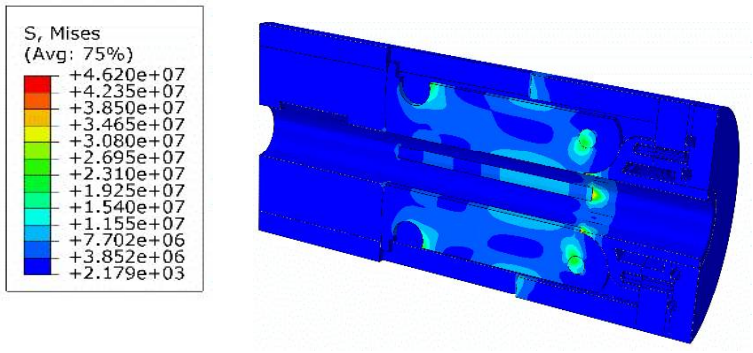

b)

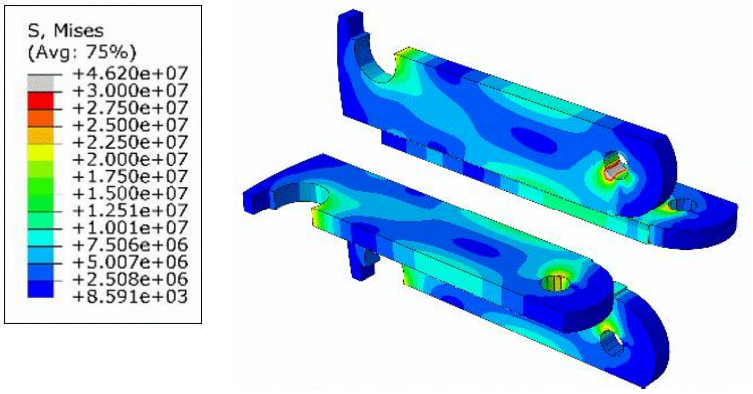

Fig. 8. Distribution of HMH reduced stress in the grooved section elements: a) general view of the model, b) structural elements in a critical stress-strain state

The maximum values of HMH reduced stress in the structural elements of the grooved section for mechanical load (pressure) were at $\sigma_z \approx 46$ MPa and were present in the material in the moving segment regulating groove depth (Fig. 8b). These values were low and posed no risk to the safe operation of the extruder's components. A significant increase in reduced stress was obtained after loading the feed section with temperature and the simultaneous application of the cooling system. HMH stress distributions in the structural elements of the extruder's grooved section, assuming continuous operation of the machine for 5 hours, are presented in Figure 9.

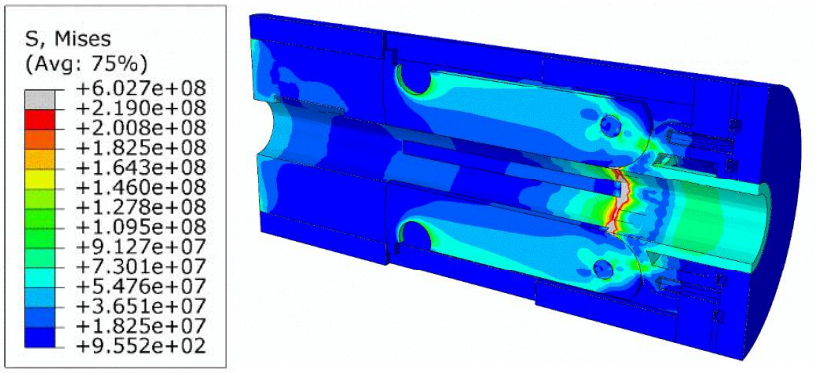

Fig. 9. Distribution of HMH reduced stress in grooved feed section elements

The introduction of thermal load into the system resulted in an increase in reduced stress to $\sigma_z \approx$ 602 MPa, in the internal sleeve body at the end zone of the grooved feed section. The observed high gradients of HMH stress in this zone pose no risk to the safe operation of the extruder, as the maximum stress was much below the assumed yield strength of $R_e = 880$ MPa. The stress levels

in the remaining structural elements of the grooved section were lower (green), facilitating uniform critical stress-strain state of the individual structural elements.

Figure 10 presents the distribution of temperatures in the grooved feed section elements after 5 hours of continuous operation of the extruder. The scale is graduated in ^{o}C.

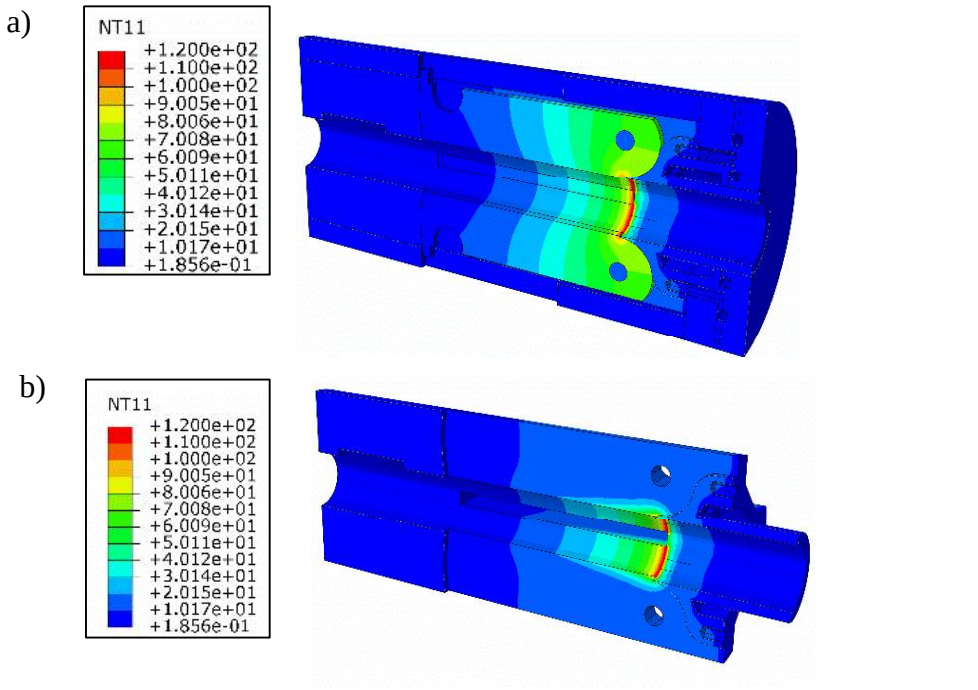

10. Distribution of temperature in the grooved section elements: a) section vi of the grooved section, b) distribution of temperatures in the internal sleeve

5. CONCLUSIONS

The maps of temperature in the grooved feed section elements demonstrate the distribution of temperature in the structure during continuous operation of the extruder. After analysing the results, one can state that the cooling system was correctly designed. This is corroborated by the temperature maps for the materials of the internal components, directly exposed to the friction temperatures generated by the transported material. The mapped temperature distribution shows that high temperatures of T = 120^{o}C were concentrated in the very narrow end area of the internal sleeve. In the remaining areas of the internal body the temperatures were low (light blue and light green) with values within the range of T = 20 – 70^{o}C. The distribution of temperature in the grooved section indicates the stable operation of the extruder, preventing premature plasticisation of the transported granulate.

The paper presents a novel design of feed section for a polymer extruder. The application of a grooved section with an option to adjust groove depth, inclination angle and number during uninterrupted extruder operation makes it possible to optimise production and improve efficiency. A numerical strength analysis of the structural elements in the extruder's grooved section was conducted with the finite element method being employed. The calculation results made it possible to verify the correctness of the extruder design in terms of strength and rigidity, assuming a production duration of 5 hours.

The calculations involved the procedure for coupled temperature-displacement, which made it possible to take into consideration the impact of friction temperature caused by the transported

granulate on the operation and strength of the extruder's structural elements. The obtained thermal analysis results corroborated the performance of the designed cooling system, with no granulate plasticisation during transport. The additional thermal barrier, which took the form of a front cooling disc, allowed the separation of the "cold" section from the plasticising (hot) section, thus facilitating optimal material transport conditions in the feed section.

The proposed concept is an innovative solution for an extruder, featuring an adjustable grooved feed section, and will be fabricated and put in production service for commercialisation purposes.

REFERENCES

[1] Sikora, J. W., Samujlo, B., Stasiek, A., Tor-Świątek, A., (2005), The mechanical properties of plasticized PVC processed in an extruder with a modified feed zone, International Polymer Processing, 30(3), pp. 359-365.

[2] Jia, M.-Y., Xue, L., Pa, P., Wang, K.-J., Jin, X.-M., (2013), Studies on the effect of pellet size on positive conveying in helically grooved single screw extruders, International Polymer Processig, 28(3), pp. 267-273.

[3] Wortberg, J., (2002), Screw and barrel design for grooved feed vs. smooth bore extruders, SPE-ANTEC, San Francisco, pp. 1-5.

[4] Sasimowski, E., Sikora, J., Królikowski, B., (2014), Effectiveness of polyethylene extrusion in a single-screw grooved feed extruder, Polimery, 59(6), pp. 505-510.

[5] Davis, B.A., Gramann, P.J., Noriega, M.P., Osswald, T.A., (2019), Grooved feed single screw extruders - improving productivity and reducing viscous heating effects, http://www.madisongroup.com/publications/spe-grooved.pdf (accessed 23 May 2019).

[6] Głogowska, K., Sikora J., Blase J., (2018), The use of untreated neuburg silliceous earth as a filler for high-density polyethylene, Tehnicki Vjesnik-Technical Gazette, 25(6), pp. 1581-1586.

[7] Zhang, Z., Cao, M., Chen, P. Yang, B., Qian, J., (2019), Improvement of the thermal/electrical conductivity of PA6/PVDF blends via selective MWCNTs-NH2 distribution at the interface, Materials & Design, 177, 107835.

[8] Sikora, J.W., Gajdoš, I., Puszka, A., (2019), Polyethylene-matrix composites with halloysite nanotubes with enhanced physical/thermal properties, Polymers, 11(5), 787.

[9] Benad, J., (2019), Numerical methods for the simulation of deformations and stresses in turbine blade fir-tree connections, Facta Universitatis-Series Mechanical Engineering, 17(1), pp. 1-15.

[10] Ming, L., Changliang, L., Qing, Z., Bing, H.,Hualin, F., (2019), Design and mechanical properties of hierarchical isogrid structures validated by 3D printing technique, Materials & Design, 168, 107664.

[11] Abaqus HTML Documentation 2018.

[12] Yang, Z.J., Harkin-Jones, E., Menary, G.H., Armstrong, C.G., (2004), Coupled temperature–displacement modelling of injection stretch-blow moulding of PET bottles using the Buckley model, Journal of Materials Processing Technology, 153-154(11), pp. 20-27.

[13] Sengupta, J., Cockcroft, S.L., Maijer, D.M., Larouche, A., (2005), Quantification of temperature, stress, and strain fields during the start-up phase of a direct chill casting process by using a 3D fully coupled thermal and stress model for AA5182 ingots, Materials Science and Engineering: A, 397(1-2), pp. 157-177.

[14] Kulkarni, S.M., Rubin C.A., Hahn, G.T., (1991), Elasto-plastic coupled temperature-displacement finite element analysis of two-dimensional rolling-sliding contact with a translating heat source, Journal of Tribology, 113(1), pp. 93-101.

[15] Bakari, H.R., Adegoke, T.M., Yahya, A.M., (2016), Application of Newton-Raphson method to non-linear models, International Journal of Mathematics and Statistics Studies, 4(4), pp. 21-31.
[16] Horiguchi, S., (2016), The Formulas to compare the convergences of newton's method and the extended Newton's method (Tsuchikura-Horiguchi Method) and the numerical calculations, Applied Mathematics, 7(1), pp. 40-60.
[17] Janicke, L., Kost, A., (1998), Convergence properties of the Newton-Raphson method for nonlinear problems, IEEE Transactions on Magnetics, 34(5), pp. 2505-2508.
[18] Verbeke, J., Cools, R., (1995), The Newton-Raphson method, International Journal of Mathematical Education in Science and Technology, 26(2), pp. 177-193.
[19] Marinković, D., Zehn, M., Milić, P., (2016), On the design of thermally loaded fiber optics feedthroughs, Thermal Science, 20, pp. S1313-S1320.

Acknowledgements

This project has received funding from the European Union's Horizon 2020 research and innovation programme under the Marie Skłodowska-Curie grant agreement No. 734205 – H2020-MSCA-RISE-2016.